J. exp. Biol. **131**, 17–36 (1987)
Printed in Great Britain © *The Company of Biologists Limited 1987*

FUNCTIONING OF IDENTIFIED SNAIL NEURONES IN ELECTRIC FIELDS

BY VICTOR N. IERUSALIMSKY

Laboratory of Molecular Biophysics, Institute of Chemical Physics, USSR Academy of Sciences, Novatorov Street 7a, Moscow, 117421, USSR

AND PAVEL M. BALABAN

Laboratory of Conditioned Reflexes, Institute of Higher Nervous Activity and Neurophysiology, USSR Academy of Sciences, Butlerova 5a, Moscow, 117865, USSR

Accepted 30 April 1987

SUMMARY

In both silent and spontaneously active neurones of the snail *Helix lucorum*, depolarization and spikes were elicited by low-frequency (0·1 Hz) sinusoidal currents applied to the bath solution. Threshold voltage gradients had a range of 1–10 $V\,m^{-1}$, which is less than gradients in the nervous tissue during synchronous activation of the neurones. It is shown that the same neurone can generate spikes in response to opposite directions of polarizing currents. Thresholds of spontaneously active neurones to extracellular currents were significantly lower than thresholds of silent cells. A simple quantitative method for evaluation of the transmembrane voltage drop evoked by an electric field is presented. The role of neuronal branches in the response was studied by electrophysiological and morphological methods.

INTRODUCTION

Extracellular voltage gradients of up to tens of volts per metre can be generated by synchronous activity of excitable cells (Jefferys, 1981). These levels are greater than the thresholds for spiking in many cases, which may be less than 1 $V\,m^{-1}$ (Terzuolo & Bullock, 1956), and can affect the precise pattern of the neuronal response, depending on the extent of that neurone which lies in the direction of the current flow (Bernhardt & Pauly, 1973). These data and related results demonstrating interactions of hippocampal neurones (Richardson, Turner & Miller, 1984) have renewed an interest in the problem of ephaptic interactions (Arvanitaki, 1942) in the brain and in the mechanisms of neuronal response to extracellular currents.

Only a small part of the extracellular current passing in the vicinity of a neurone will cross the membrane to flow intracellularly. The resulting transmembrane current depends largely on the morphological features of the nerve cell. However, the current that does enter the cell will enter through regions closer to the positive pole of the extracellular potential dipole, causing a hyperpolarization of such regions, and

Key words: extracellular current, molluscan neurone, transmembrane voltage gradient.

leave closer to the negative pole, where it will result in a depolarization. Passing of transmembrane current through an intracellular electrode will cause only one type of polarization in the whole cell: either hyperpolarization or depolarization, depending upon current polarity. The difference between cellular reactions to the extracellular and intracellular current is of great importance for understanding mechanisms of neuronal functioning in electric fields.

In a number of investigations it has been shown that extracellular current can modulate cellular activity in hippocampus (Jefferys, 1981), cerebellum (Granit & Phillips, 1957) and cortex (Bindman, Lippold & Redfearn, 1964). Unfortunately, almost all the available quantitative data are approximate due to strong heterogeneity of extracellular current. The best quantitative data are presented in a classic paper by Terzuolo & Bullock (1956). In this work the threshold of neuronal reaction to an extracellular homogeneous electric field was evaluated ($1\ V\ m^{-1}$), and the nature of the neuronal response was considered. Theoretical analysis shows that the integral shift of transmembrane potential in the cell in low-frequency extracellular current must be zero, but it was experimentally established that the neurones respond with spikes to extracellular current. The mechanism of this response has not been examined in detail.

The present communication describes the electrical responses of identified neurones, with known morphology, to the influence of extracellular current.

MATERIALS AND METHODS

Experiments were carried out on giant identified neurones (soma diameter up to 250 μm) of the snail *Helix lucorum* L. The location of the neurones on the dorsal surface of the suboesophageal ganglia complex and pedal ganglia is shown in Fig. 1. Isolated ganglia were pinned with cactus pins to the wax floor of a round chamber filled with snail saline (Sacharov, 1974). Two Ag–AgCl rectangular macroelectrodes (12×15 mm) were mounted in the chamber, 14 mm apart, on either side of the nervous system, and their position could be changed gradually in one plane (Fig. 2). The maximal length of the nervous system preparation was 8–10 mm. After dissection of the ganglia sheath, the nervous system was bathed in 0·2% papain (Merck) for 15 min. The remaining connective tissue covering the identified neurones on the dorsal surface was removed with fine forceps. In all experiments the location of the nervous system in the chamber was identical.

Unless otherwise mentioned, a sinusoidal electric field with a frequency of 0·1 Hz was used in all experiments. This frequency was adopted because in preliminary experiments it had been established that, at frequencies greater than 1 Hz, some cells do not respond to every half-wave of the sine current, while at frequencies of less than 0·05 Hz some accommodation is seen. The optimal frequency of extracellular current for the large (150–250 μm diameter) snail neurones was approximately 0·1 Hz.

Outlines of the experimental set-up for intracellular or extracellular stimulation and the equivalent circuit are presented in Fig. 3. Stimulating current was controlled

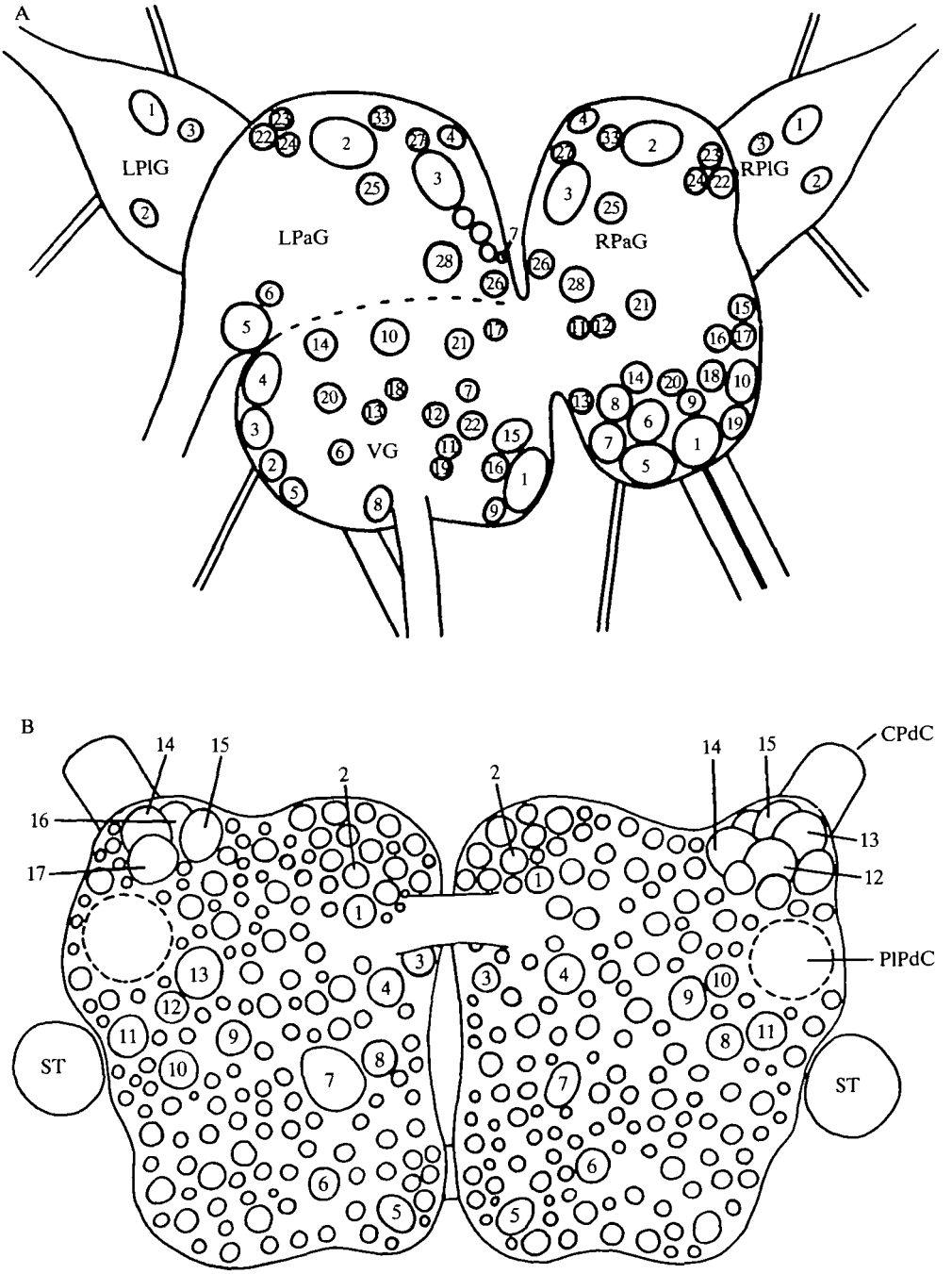

Fig. 1. Schematic representation of neuronal localization on the dorsal surface of the suboesophageal ganglia complex (A) and on the dorsal surface of the pedal ganglia (B). LPlG and RPlG, left and right pleural ganglia; LPaG and RPaG, left and right parietal ganglia; VG, visceral ganglion; ST, statocyst; CPdC, cerebropedal connective; PLPdC, pleuropedal connective. Identifiable neurones are numbered.

by measuring the voltage drop on a series resistor of 10 Ω (R_t in Fig. 3). Usually current had a range of 0·01–6·5 mA (0·005–3·6 mA cm^{-2}), corresponding to a voltage gradient of the order of tens of volts per metre.

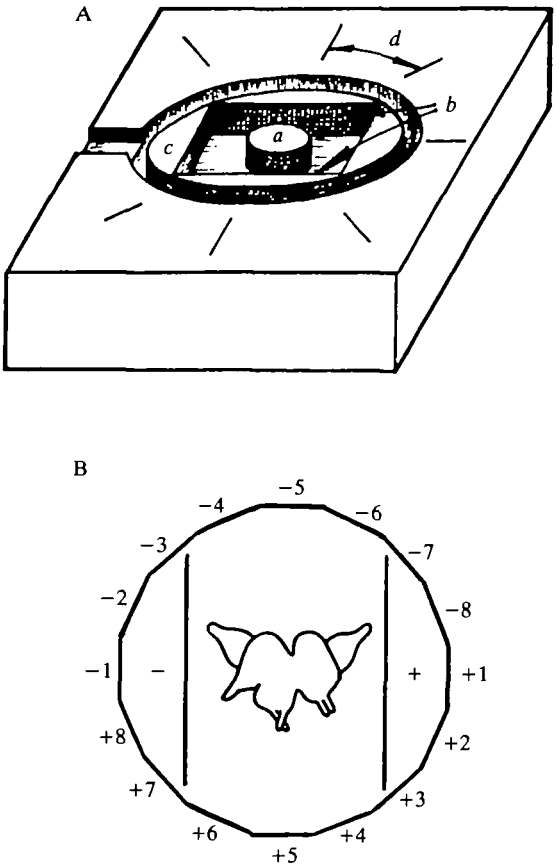

Fig. 2. Schematic view of the round fluoroplastic experimental chamber (A) and eight positions of the macroelectrodes in relation to the usual position of the CNS (B). *a*, column on which CNS is placed; *b*, rectangular Ag–AgCl macroelectrodes; *c*, a round fluoroplastic inset on inner surface of which macroelectrodes are glued; *d*, marks of macroelectrode position. In B eight positions of the macroelectrodes are numbered. The grounded electrode is marked with a minus. The real dimensions of the macroelectrodes in relation to the CNS dimensions are shown in the centre.

Fig. 3. Equivalent circuit (A) and schematic representation of experimental device (B). V, total drop of potential across the experimental chamber; R_c, resistance of metal–solution transition; R_1, R_2, saline resistance over dimensions d_1 and d_2; R_a, saline resistance over dimension of the cell (a); R_t, testing constant resistance, 10 Ω; R_{in}, input resistance of the neurone; R_e, microelectrode resistance; R_A, input resistance of the amplifier; I_o, current in the experimental chamber; I_1, I_2, currents through the polar, relative to the macroelectrodes, parts of the neurone; I_3, current through R_a; I_4, current through R_t; I_5, current through the intracellular microelectrode; St, current stabilization; G, generator of sine-wave signal; S, generator of square wave impulses; P, plate macroelectrodes; A_1, A_2, A_3, amplifiers; d_1, d_2, distance from the 'poles' of the cell to the macroelectrodes; a, cell dimension in the current direction.

Conventional electrophysiological methods were used for intracellular recordings. Glass recording micropipettes had tips of 0·5–1·0 μm in diameter and contained 2 mol l^{-1} potassium citrate. To make intracellular recordings in the presence of an

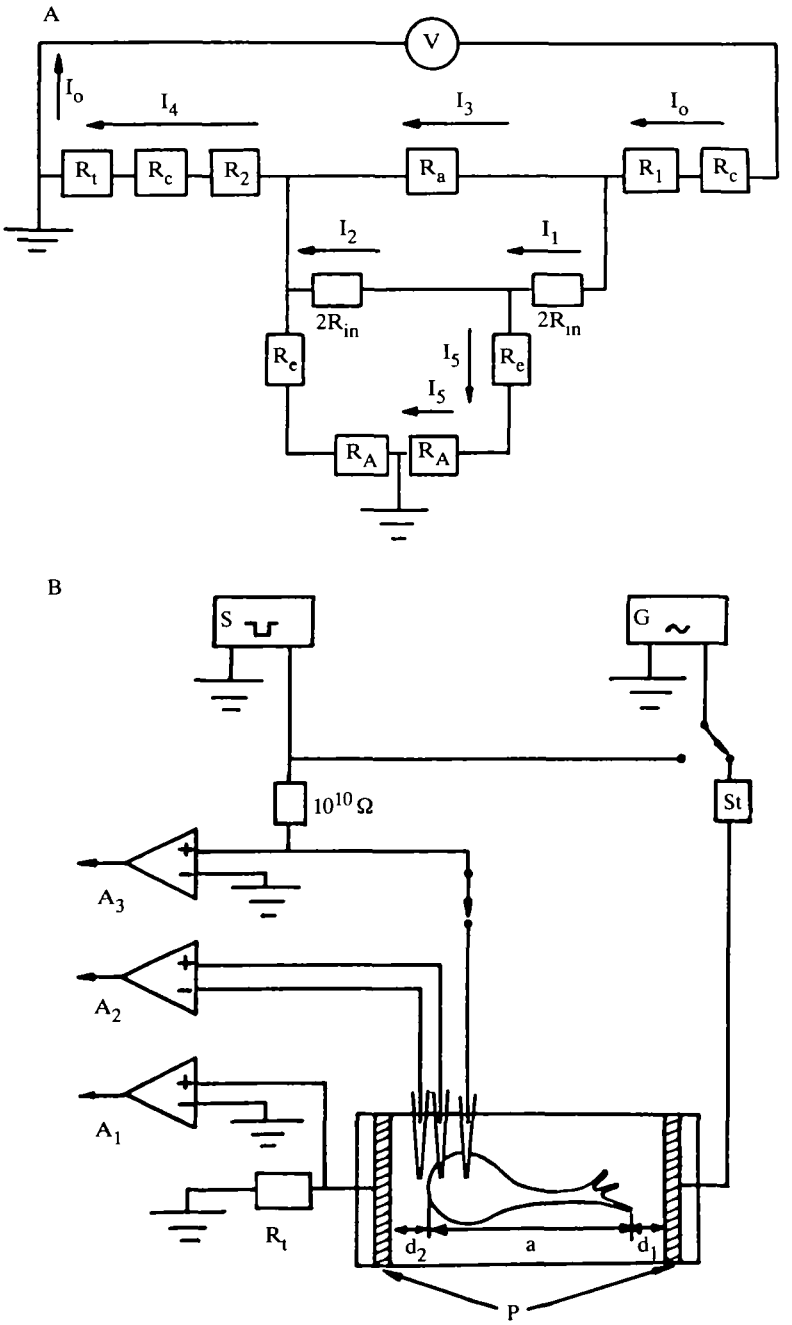

Fig. 3

extracellular electric field, it was necessary to use a differential input amplifier (A_2 in Fig. 3). Input resistance of the amplifier was $10^{11}\,\Omega$. The recording electrode was connected to the positive input of the amplifier, while the reference electrode was placed (unless specified) near that region of the somatic membrane which was closest to the pole of the extracellular voltage gradient. The distance between the reference electrode and the membrane was measured using the calibrated eyepiece of the microscope.

Intracellular current injection was made using a second intracellular microelectrode. Neuronal activity was recorded on an oscilloscope and on a rectilinear pen-recorder.

In experiments with large extracellular current it is essential to know if a part of this current is flowing through the intracellular recording microelectrode. Inward (I_1) and outward (I_2) transmembrane currents can be approximately defined by the formulae:

$$I_1 \approx \frac{I_o}{4}\left[\frac{R_a}{R_{in}} + \frac{2(R_t + R_c + R_2)}{R_A}\right],$$

$$I_2 \approx \frac{I_o}{4}\left[\frac{R_a}{R_{in}} - \frac{2(R_t + R_c + R_2)}{R_A}\right],$$

where I_o is the total current through the chamber, R_c is the resistance of the electrode–saline interface, R_2 is the resistance of the saline for the distance d_2 from the neurone to the grounded macroelectrode (Fig. 3), R_a is the resistance of the saline for the length a (on Fig. 3) of the neurone, R_{in} is the input resistance of the cell and R_A is the input resistance of amplifier A_2. It can be seen from the formulae that only when R_a/R_{in} is much greater than $2(R_t + R_c + R_2)/R_A$ can the current flowing through the microelectrode (I_5) be neglected. In our experiments R_a ranged from 1 to $10\,\Omega$, R_{in} was about $10^7\,\Omega$ and $2(R_t + R_c + R_2)$ was not greater than $10^3\,\Omega$. This means that R_A must be greater than $10^{10}\,\Omega$ (and was actually $10^{11}\,\Omega$). The second intracellular microelectrode amplifier had an input resistance of $10^{10}\,\Omega$ and was switched off during application of extracellular current (Fig. 3).

In all experiments the recording electrode was inserted in the soma. The second intracellular electrode was also inserted in the soma, except for left pedal neurones 7 and 8, where it could be inserted in branches near the ganglion surface. Unless mentioned otherwise, the reference electrode was placed extracellularly near that pole of the soma which was closer to the macroelectrode. In some experiments this electrode was moved along the surface of the cell. In every experiment the voltage gradient in the external solution was measured using two microelectrodes placed in the solution at a known distance apart.

It is not possible to avoid some polarization of the plate electrodes during current flow even if they are covered with AgCl. In an attempt to control some effects of polarization, pH was measured, to an accuracy of 0·01 unit, in the centre of the bath, where the ganglia were located. No measurable changes of pH were seen after 5 min of 5 mA sinusoidal current.

In most experiments the morphology of the impaled neurone was investigated after the recording by inserting a microelectrode filled with 3% Lucifer Yellow (Sigma) into the same cell. Lucifer Yellow was injected ionophoretically using hyperpolarizing current impulses (6 nA, 450 ms with a frequency of 2 Hz for 1–2 h). After this procedure the whole nervous system was fixed in 4% formaldehyde buffered with a phosphate buffer (Kater & Hadley, 1982) for 10 min followed by fixation in 4% formaldehyde in absolute ethanol for 1 h. The preparation was cleared in methylbenzoate for 10 min before making a whole-mount.

RESULTS

The 'effective length' of the neurone, and the voltage gradient induced by extracellular current

The voltage gradient induced by extracellular current in the nerve cell was investigated in detail in 12 experiments in which the recording electrode was located above the soma of the neurone (position 2 in Fig. 4), then inserted into the cell (position 2″) without changing its position in relation to the macroelectrodes. As the electrode was inserted, there was a large increase, decrease or even change in polarity in the voltage gradient observed between the recording and reference electrodes (Fig. 4B). Both in neurones with processes many times longer than the soma (Fig. 4Ai) and in neurones with relatively short processes (Fig. 4Aii), it was found that the position of the reference electrode affected the amplitude and polarity of the recorded voltage (Fig. 4B) but did not affect the spikes evoked by the extracellular current (Fig. 4C).

The electrical potential generated on the neuronal membrane could be measured by placing the recording and reference electrodes in the plane perpendicular to the current direction (Fig. 5Bii). The extracellular voltage gradient between the electrodes was approximately zero (Fig. 5Cii). When the recording electrode was inserted, the membrane potential was observed, and spiking was exhibited in response to one polarity of the extracellular current (Fig. 5Aii). It should be noted that these spikes could be recorded with an extracellular electrode, and insertion of a microelectrode into the soma did not change significantly the number of spikes in the response (data not shown).

It was found that the reference electrode could be placed at a distance from the soma such that the sinusoidal deflections recorded by the intracellular electrode were minimal (Fig. 5Aiv). In the case of unipolar identified neurones, the location of the reference electrode was always observed to be along the line of the axon. With the reference electrode at this point, large deflections in voltage were observed when the recording electrode was in an extracellular position (Fig. 5Civ).

In giant pedal cells 7 and 8 it was possible to insert intracellular electrodes in the axons (30–40 μm in diameter) due to their location on the ganglion surface (Fig. 6). With the reference electrode at a constant location, the voltage gradient induced by the extracellular current was the same with the intracellular electrode in the soma as

it was with the electrode in the axon at a distance of hundreds of micrometres from the soma. This result suggests that the voltage gradient inside the neurone differs from the voltage gradient in the surrounding saline and is very small. This was confirmed by recording simultaneously from the soma and the axon of the same cell with a distance between the electrodes of 300–500 μm (Fig. 7). It was established that the voltage gradient in the cell was 30–70 times smaller than the voltage gradient at the same distance in the saline. Taken together, these results lead to the conclusion

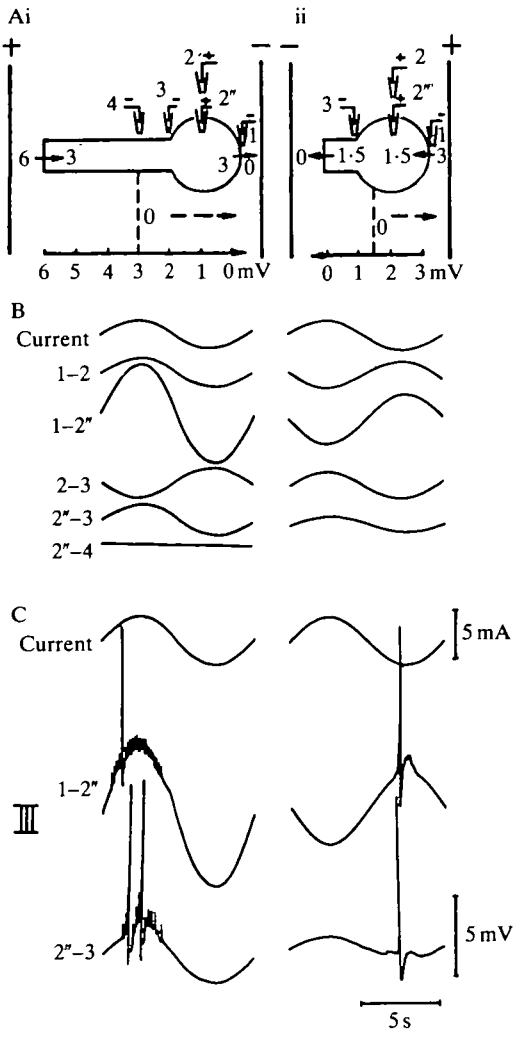

Fig. 4. Reactions of two neurones with different effective lengths to subthreshold (B) and suprathreshold (C) extracellular current. (A) Schematic representation of electrode position, extracellular current direction, and induced potential. (i) Data from a cell with a relatively long process; (ii) data from a cell with a relatively short process. 1, 2, 3, 4, 2″, electrode number. In B and C the number of both recording electrodes is shown on the left-hand side. The dotted line with the arrowhead shows the direction of the induced current that is evoking spikes.

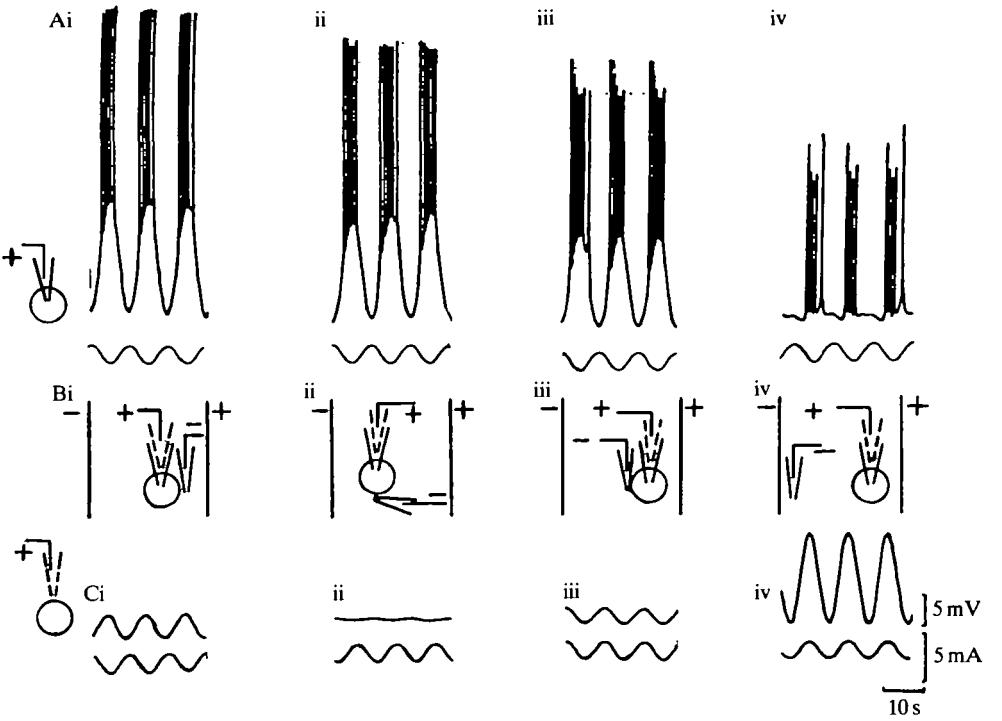

Fig. 5. The dependence of the potential recorded in cell RPa5 upon the position of the extracellular electrode. (A) Intracellular recording (current in all cases is shown on lower trace); (B) schematic representation of electrode position (dotted electrodes correspond to records in C); (C) recording of electric field with two extracellular electrodes. Distance between electrodes in Biv is 1·2 mm. (i–iv) Recordings with extracellular electrodes positioned differently.

that, in a neurone placed in an electric field, a major voltage drop can be recorded at the membrane in the zones where maximal input and output currents flow.

The direction of currents evoked in the neurone by the extracellular electric field is indicated schematically for three different cell types in Fig. 8. The typical monopolar molluscan neurone is represented by a soma and a process of large diameter (left-hand model on Fig. 8A). Extracellular current applied along the direction of the cellular process flows extracellularly and only a small fraction flows intracellularly. The equivalent electrical circuit (Fig. 8B) consists of the resistances of extracellular fluid (R_{out}) and intracellular fluid (R_{int}), and resistances of the cellular membrane to the input current (R_{m1}) and output current (R_{m2}). Taking into consideration the fact that membrane resistance is many times greater than cytoplasmic resistance ($R_{m1} \gg R_{int}$; $R_{m2} \gg R_{int}$), the cell can be represented by an ellipsoid ($R_{m1} \approx R_{m2}$). The voltage drop in the cell would be maximal across R_{m1} and R_{m2}, being near zero across R_{int}. The potential induced in a cell placed in an electric field is equal to the voltage gradient along the length of the cell (Bernhardt & Pauly, 1973). This means that the voltage drop across both R_{m1} and R_{m2} would be greater with an increase in the cell's length and equal to the voltage gradient on the half-cell dimension. Integral induced

potential of the cellular contents (if one neglects voltage drop on R_{int} as well as the resting potential of the membrane) would be equal everywhere in the neuronal interior, and can be calculated as the potential of a point in the middle of the cell. These considerations easily explain the observations presented in Figs 4 and 5. The middle of the neurone is the 'zero point' for the induced potential. This notion helps us to compare experimental data (Fig. 4A; Fig. 5) with theoretical considerations (Fig. 8). For a neurone of the typical shape, the soma can be considered as one pole of a dipole induced in the cell by the electric field. Also, the current directed from the soma to the process hyperpolarizes the whole soma (and *vice versa*). The greatest polarization is in the regions of the soma which are closest to the macroelectrodes generating the electric field ('poles' of the soma).

A neurone with a relatively short axonal process will show some polarization of the soma when it is in the electric field (Fig. 8A, centre) while a soma without a process will be depolarized on one side and hyperpolarized on the other (Fig. 8A, right).

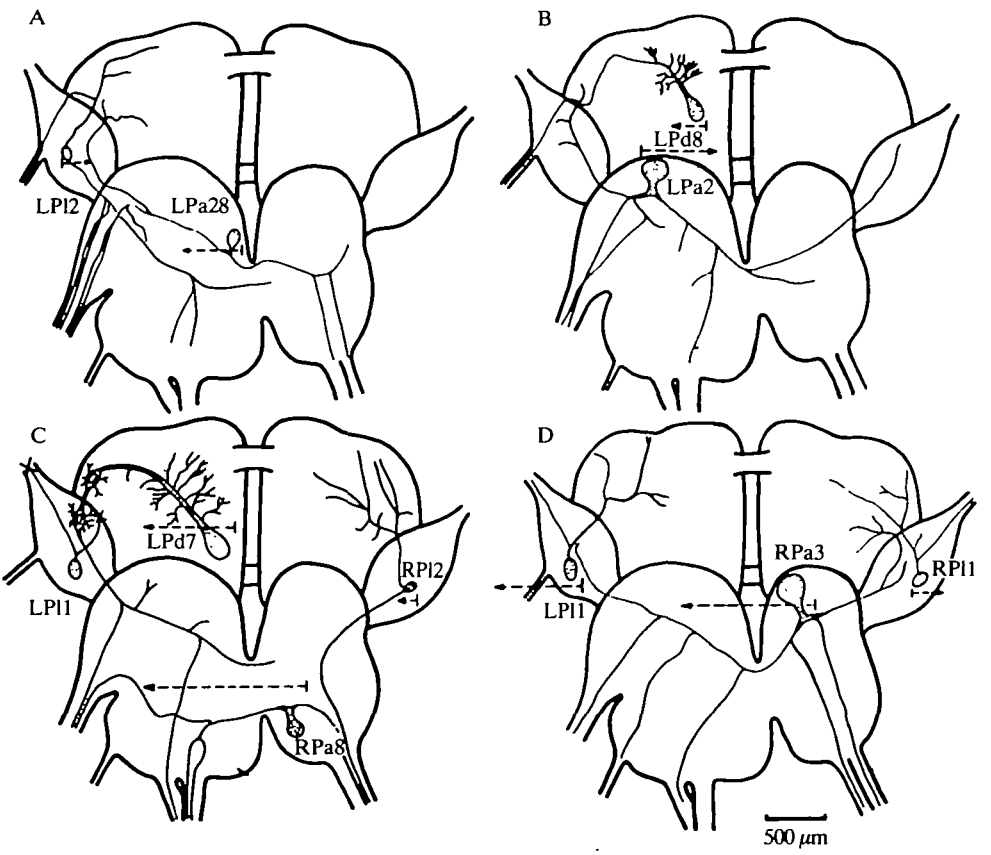

Fig. 6. Morphology of some identified neurones revealed by Lucifer Yellow after the electrophysiological experiments. Dotted lines with arrowheads show the amplitudes of the effective length (see text for explanation) of the cell with the macroelectrodes in position 1.

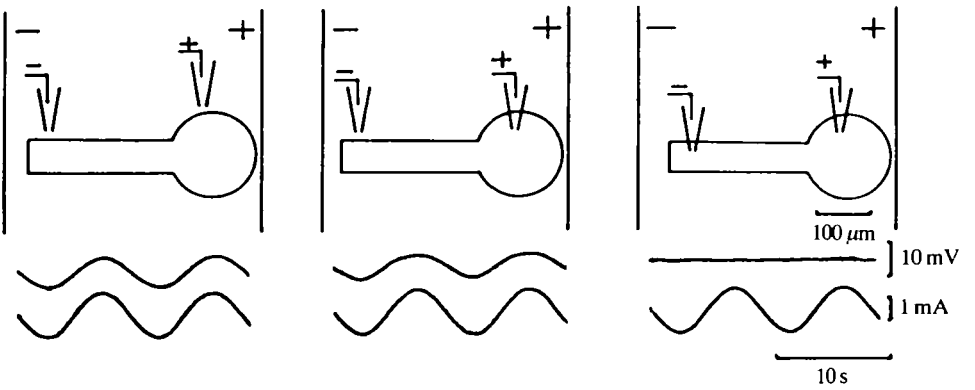

Fig. 7. Changes of the electric field amplitude after insertion of one microelectrode into cell LPe7 (in the middle) and after insertion of both recording electrodes into the cell (on the right). The position of the electrodes is shown at the top of every record. Upper trace, electric field recorded by electrodes; lower trace, current in the saline. Macroelectrode positions relative to the main process of cell LPe7 are shown.

It is evident that for correct interpretation of neurophysiological results the morphology of identified neurones must be taken into consideration. Only monopolar neurones, where the soma is one pole of a dipole, are represented in the model (Fig. 8) and branching is not represented. A series of experiments was carried out to investigate the applicability of this simple model.

Cell LPl1, sending branches in the pleuropedal and pleurocerebral connectives (see Fig. 6D), was investigated in detail in six snails. The voltage gradient induced by extracellular current was measured in the soma before and after ligating the connectives at a distance of 650–1450 μm from the soma. The effectiveness of separation of remote branches was controlled by checking that Lucifer Yellow injected into the cell did not pass the ligature. It was established that such 'shortening' of a neurone had no noticeable influence on the voltage gradient in the soma induced by extracellular current. This suggests that small, remote branches do not contribute significantly to the voltage gradient recorded in the soma, and that the proximal part of the process contributes most to the cellular reaction. This was shown in experiments in which simultaneous recordings were made from both pleural neurones (LPl1 and RPl1). The proximal part of a single process in each of these cells leaves the soma almost in opposite directions (to the left in LPl1, to the right in RPl1; see Fig. 6). This suggests that the reaction of the soma in the left cell must be evoked (by the extracellular current) simultaneously with the reaction of the process in the right neurone. Indeed, it was established experimentally that axonal spikes as well as somatic spikes are evoked in either cell by extracellular current of the opposite direction (Fig. 9).

The single process leaving the soma forms two branches in some neurones (e.g. RPa3, see Fig. 6). If these two branches were distributed symmetrically in opposite directions, it would be expected that the potential induced in the soma by extracellular current would be near zero. In 117 preparations it was established that

an induced potential can be recorded in the soma, presumably due to non-symmetrical branching.

The potential differences generated in electric fields at the ends of a neurone with branching processes cannot be equal in different branches. The potentials of the poles in the distal processes will be greater than the potentials in the soma (because the process resistance – R_p in Fig. 8B – is much greater than the soma resistance, R_s).

It seemed useful to introduce the term 'effective length' of the cell. Assuming that the voltage drop across the somatic membrane represents half of the voltage drop over the whole length of the cell in the direction of the electric field, we define the effective length of the cell to be equal to twice the distance over which the voltage drops to the value recorded in the soma. In other words, the effective length of a given neurone is the length of a symmetrical dipole with a potential equal to that recorded in the soma of this neurone. The 'zero point' is in the middle of such a dipole. Potential induced in a protracted ellipsoidal cell by a low-frequency electric field can be estimated using the equation: $U = Ea/2$, where U is the maximal

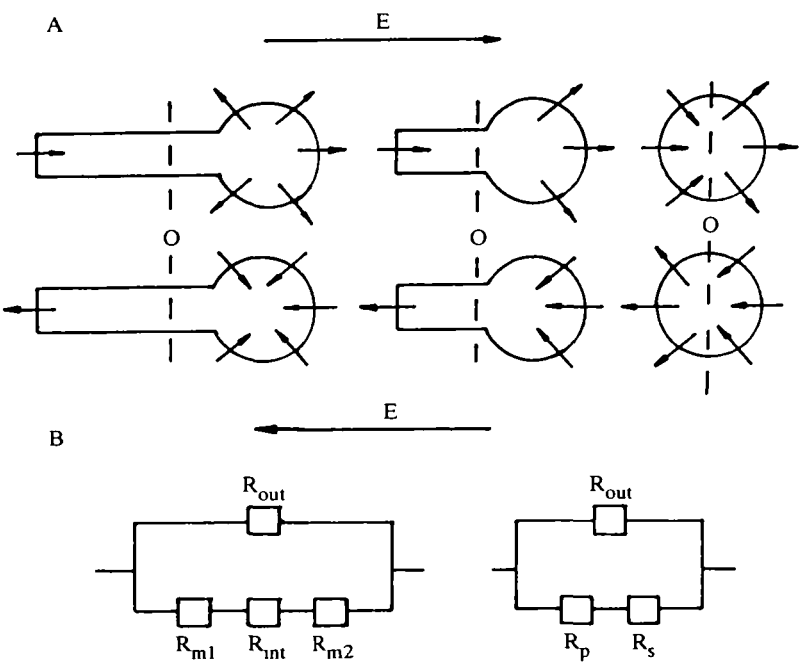

Fig. 8. Types of polarization of the cell in the electric field (E) in relation to the effective length (A) and two equivalent circuits (B). (A) Left, effective length much longer than the soma diameter; middle, effective length equal to two soma diameters; right, effective length equal to soma diameter. The arrows (E) show the direction of the extracellular electric field for the upper and the lower schemes; the dotted line marks the centre of the cellular dipole. (B) Simplified equivalent circuits of a neurone with a large process (left) and of a neurone with a long, thin process (right) in the extracellular electric field. R_{out}, resistance of the extracellular saline at a dimension of the neurone; R_{int}, resistance of the neuronal internal medium; R_{m1}, R_{m2}, resistances of the neuronal membrane at the place of exit and entrance, respectively, of the extracellular current; R_p, resistance of the process; R_s, soma resistance.

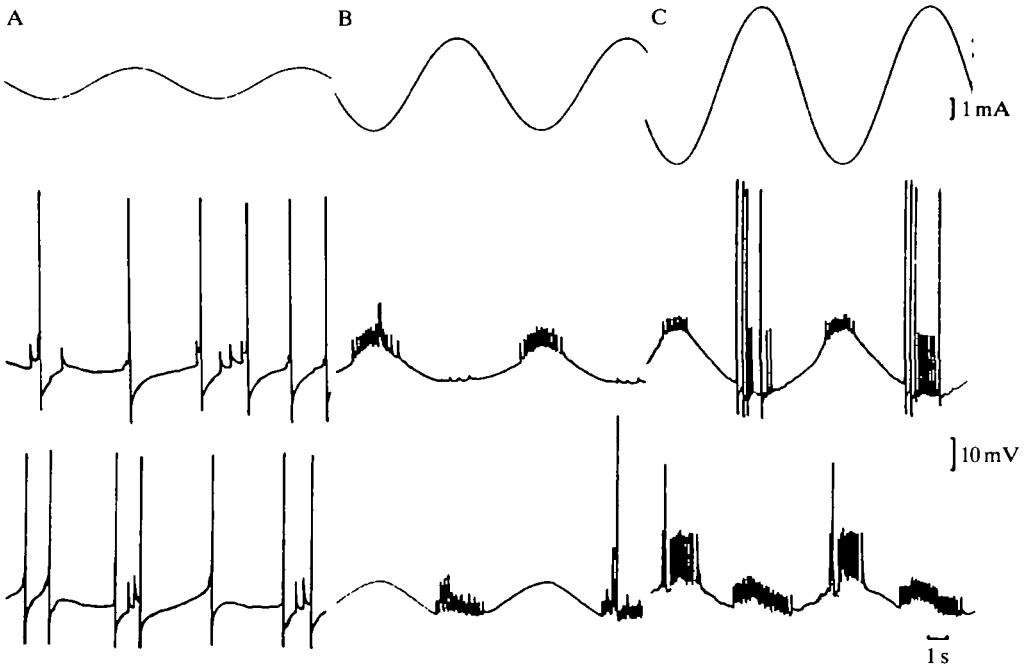

Fig. 9. Reactions of symmetrical (left and right) giant neurones from pleural ganglia (RPl1, middle trace, and LPl1, lower trace) to the extracellular current (upper trace). Macroelectrodes in position 1. Extracellular current increases from A to C.

potential induced across the somatic membrane, E is the voltage gradient in solution and a is the length of the cell in the direction of the electric field (Bernhardt & Pauly, 1973). If it is experimentally possible to measure independently both U and E, then the effective length of the cell can be estimated. The effective lengths of the same identified neurones from different specimens, and of cells with differing morphology, can provide additional information about the reactions of neurones to extracellular current.

Soma diameters and effective lengths of investigated neurones are shown in Table 1. In most cases the effective length was greater than the soma diameter (up to

Table 1. *Maximal effective length of investigated neurones*

Neurone	Mean diameter (μm)	Type of neurone silent/SA	Number of animals	Maximal effective length (μm)
LPl1	130 ± 14	silent/SA	9	766 ± 160
LPa28	125 ± 16	silent	8	817 ± 155
RPa3	195 ± 19	silent	5	1041 ± 198
LPa3	213 ± 16	silent	4	791 ± 107
LPe7	225 ± 25	SA	4	820 ± 75

SA, spontaneously active neurone; maximal effective length, averaged for all preparations, was estimated by changing the direction of the suprathreshold electric field (frequency = 0·1 Hz). Standard error of the mean is given for every averaged parameter.

10 times), but in all neurones the morphologically evaluated length of the branches (see Fig. 6) was many times greater than the effective length. These data confirm the suggestion that the contribution of remote branches is very small, but that proximal parts of the cell processes make an essential contribution to the current-induced voltage gradient.

The effective length of the cell largely depends on the direction of the electric field, and is indicated in vector form in Fig. 6. Note that the direction of maximal effective length in all experiments coincides with the direction of the major process.

The measurements of effective length (Table 1) depend upon the assumption that there is a uniform field around the neurones. The current flow in the extracellular space within a ganglion can be non-uniform, producing local currents stimulating the cell. To assess this influence, the effective lengths of 24 identified neurones with long processes (sometimes branching) were measured before and after mechanical extraction from a ganglion treated with 1 % pronase (Sigma) for 60 min. If the process was significantly long (more than four times the diameter of the soma), the effective length was unaffected by the extraction. Also, the effective length corresponded well with the real length of the cell which was measured visually. These data support our results for cells within a ganglion. It is possible that the extracellular geometry has little effect because the cells in the enzyme-treated ganglion are loosely packed, compared, for example, to cells of the vertebrate brain.

The dependence of the threshold on the direction of the extracellular current

It is evident that the position of the macroelectrodes must affect the distribution of the current-induced potential in the cell, and it was established that the threshold current (estimated for the silent neurones as the minimal intensity of extracellular current needed for generation of one somatic action potential) can change up to 10 times with the change of macroelectrode position.

When the macroelectrodes were rotated around the nervous system, it was observed that the current-induced potential did not always exhibit the same waveform as the extracellular current, but could be distorted and show frequency-doubling (Fig. 10). Spikes which occurred near the peak of the depolarizing wave indicated that the distortions of the waveform were due to active generation of potential in different loci of the membrane.

In most experiments it was possible to record spike responses to both directions of sine-wave extracellular current, and in all studied cells changing the position of the macroelectrodes elicited significant, and reversible, alterations of response (Fig. 11).

The excitability of the soma of silent neurones was 'scanned' in 16 experiments by measuring the threshold of the spike reaction to current applied from each of eight positions (Fig. 2). For every position the current intensity evoking one spike in response to one direction of the extracellular current (first threshold) and to the opposite direction of current (second threshold) was measured at least five times. It was established that the effective length of the identified cells depended on the position of the macroelectrodes, and the maximal value could be 10 times greater than the minimal value in one experiment. Minimal effective length was usually close

to the soma diameter, while maximal effective length reached 1700 μm. Minimal first spike threshold current (in extracellular solution) for the silent cells was 0·2 mA, and maximal first spike threshold current was 5·0 mA. Second spike threshold current ranged from 0·3 to 6·5 mA. Dependence on macroelectrode position was characteristic for threshold current.

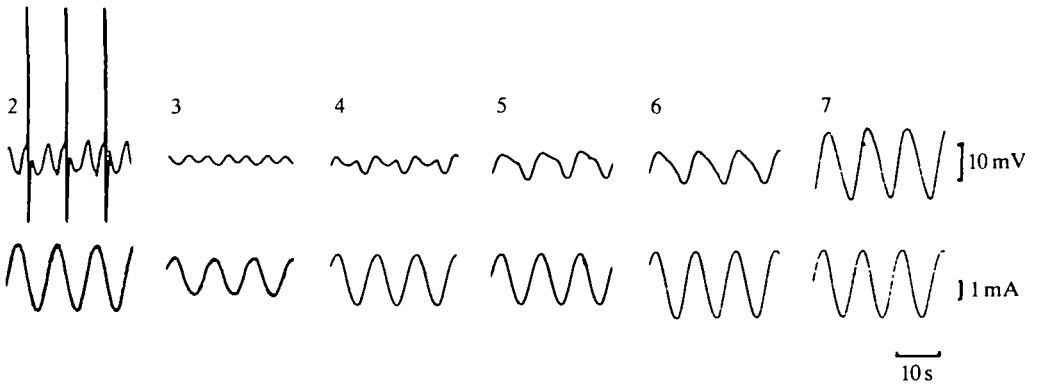

Fig. 10. Changes in waveform of intracellularly recorded potentials in LPa3 in relation to the direction of the extracellular current (lower trace). Figures indicate the position of the macroelectrode (see Fig. 2).

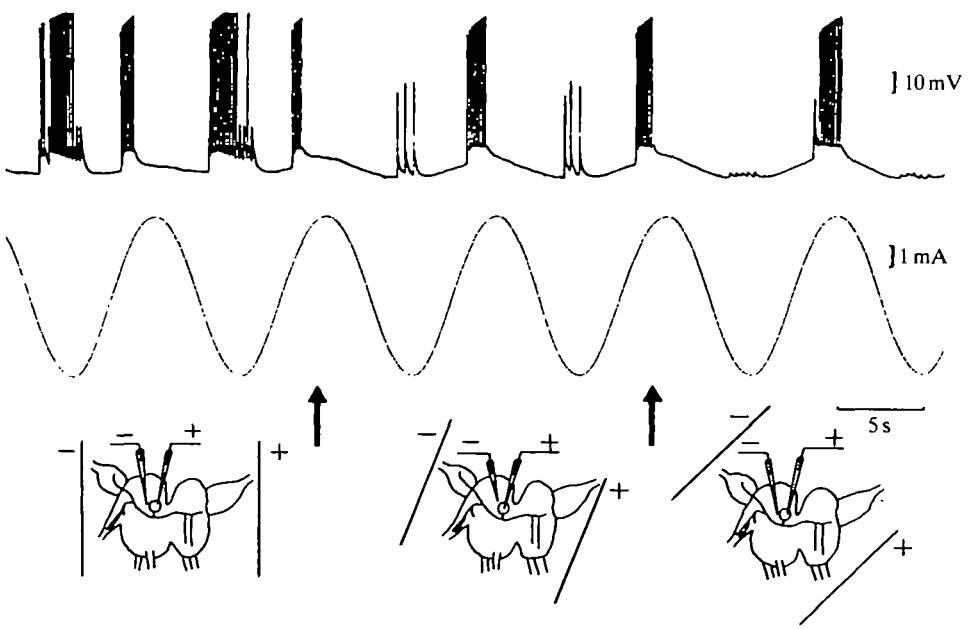

Fig. 11. Changes in the pattern of the reaction of cell LPa28 (upper trace) caused by a change of extracellular current (lower trace) direction. The position of macroelectrodes is shown at the bottom. Arrows indicate the moment when the macroelectrode position is changed.

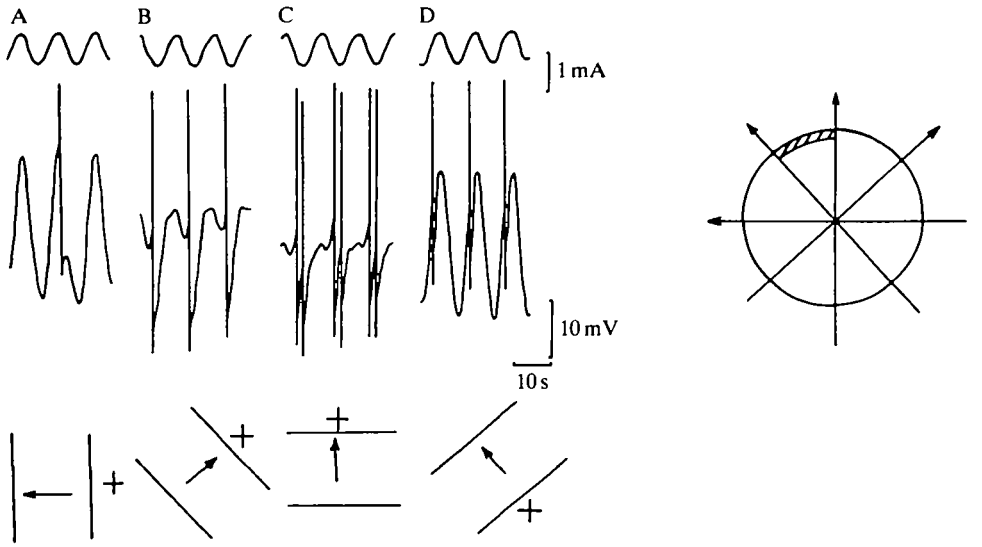

Fig. 12. 'Scanning' of the somatic membrane by extracellular currents (upper trace in A–D) of different direction (shown at the bottom). The intracellularly recorded response of neurone RPa3 is shown in the lower trace in A–D. A diagrammatic representation of the soma is shown on the right. The zone of minimal threshold is marked. Arrows indicate current direction.

The zone for minimal threshold of spike generation generally corresponded to the place where the process leaves the soma. Axonal spikes are usual for this zone (Fig. 9). The second zone (a somatic one, with higher threshold) was discovered in a number of experiments (Fig. 12). For some areas of somatic membrane the threshold for spike generation was 10 times greater than the minimal threshold.

The reaction of spontaneously active neurones

The reaction of spontaneously active neurones to the extracellular current was variable (Fig. 13). In 46 experiments (using 22 identified cells), with macroelectrodes in position 1, two types of reaction were noted as characteristic. These reactions were an increase of spontaneous activity in response to both directions of extracellular current, and an increase in response to one direction and a decrease in response to the other. Minimal threshold for spontaneously active neurones was 0·1 mA (1·3 V m^{-1}).

In 11 preparations, spontaneous firing at low frequency (0·2–1 Hz) was disturbed by near-threshold extracellular current, and the cell stopped firing. Further increases of extracellular current elicited phase-locked spikes, and then sometimes led to the disappearance of spikes in response to one direction of extracellular current. Characteristic for all spontaneously active neurones was long-lasting impairment of spontaneous spike frequency after the influence of extracellular current, presumably due to the after-effects. These reactions of spontaneously active neurones to electric field influence are not illustrated because they are qualitatively similar to the reactions for silent neurones, and tend to be obscured by spontaneous firing.

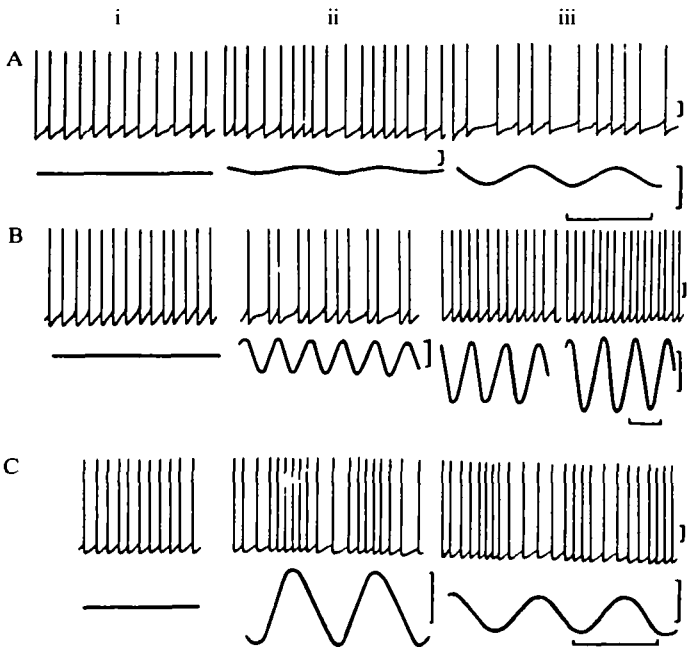

Fig. 13. Reactions of spontaneously active neurones LPl1 (A), V8 (B) and V20 (C) to intracellular (ii) and extracellular (iii) currents. (i) Spontaneous activity. Current is shown in the lower trace in all cases. Calibration bars: 10 s, 10 mV, 1 mA (extracellular current), 5×10^{-11} A (intracellular current).

DISCUSSION

In neurones placed in an electric field, potentials were induced that depended on the neurone's dimensions and the distribution of branches. The induced potential was different in the soma and in the processes, and depended on the direction of extracellular current. The intracellular voltage gradient was many times smaller than the extracellular voltage gradient. These observations confirm the previous suggestion of the existence of an intracellular voltage gradient (Terzuolo & Bullock, 1956), and the idea that in an electric field the cell can be considered as a dipole (Terzuolo & Bullock, 1956; Bernhardt & Pauly, 1973). The potential induced in such a dipole will be maximal at the poles and zero in the middle. It must be noted that in the giant neurones of the snail, the processes of which branch in various directions, the dipole induced in the cell is asymmetrical. The soma usually represents one pole. The second pole is not localized, but is distributed in branches of the cell. The dipole is not symmetrical because the input resistance of the small branches is significantly higher than the input resistance of the soma. Quantitative description of such a dipole is difficult, and we have introduced a concept of effective length, defined as the length of a symmetrical dipole with the potential at the poles equal to the maximal potential recorded in the soma of a given neurone. The effective length of a neurone changes with a change of electric field direction.

Some peculiar properties of the neuronal response to the electric field were discovered in our experiments which were not predicted by the model. It was

established that during the influence of sine-wave extracellular current it was possible in some conditions to record induced intracellular potentials of another waveform and even of doubled frequency (Fig. 10). It is assumed that these distortions of induced potential were due to the active generation of current in local depolarized areas with low threshold. This was proved by the demonstration that the distortions were greatly diminished by a change in electric field direction. Our assumption is that the heterogeneity of neuronal membrane excitability is the cause of these distortions, considering the fact that the integral intracellular potential of a cell with homogeneous membrane in an electrical field is presumed to be zero (Terzuolo & Bullock, 1956).

When the effective length is significantly greater than the soma diameter, the entire soma should be hyperpolarized by one direction of extracellular current. Nevertheless, somatic action potentials were recorded in such experiments in response to both directions of extracellular current (Fig. 9A). This contradicts experiments reported for vertebrates and invertebrates in which antidromic action potentials are blocked near the soma (Tauc, 1962*a*,*b*; Tauc & Hughes, 1963), and in which it is presumed that this blockade is due to differences in geometry of axon and soma (Coombs, Curtis & Eccles, 1957*a*,*b*). It is possible that in the case of electric field influence some additional mechanisms must be taken into consideration.

Ephaptic interactions in the brain are still not understood. Some investigators consider ephaptic interactions in the brain to be possible (Jefferys, 1981; Creutzfeldt, Fromm & Kapp, 1962), but experimentally they have been shown only in muscles (Brown & Matthews, 1960), hippocampus (Richardson *et al.* 1984) and the Mauthner cells of goldfish (Furukawa & Furshpan, 1963), and they are possible between axons included in one nerve only when the velocity of impulse conduction is decreased or the resistance of the extracellular fluid is increased (Ramon & Moore, 1978). The threshold values of neuronal reactions to the electric field have been estimated in our experiments for the giant cells, the dimensions of which are about 10 times greater than the dimensions of vertebrate neurones. The dimensions of the cell determine the amplitude of the potential induced by extracellular current. This means that for extrapolation of our results to vertebrate neurones the threshold value must be increased 10-fold, and will reach 15–300 V m^{-1}. An electric field of 30 V m^{-1} is observed in the intact brain of vertebrates (Jefferys, 1981), which suggests that ephaptic interaction in the brain is possible.

Although the ionic currents underlying action potentials have been shown to be different between soma and axon (Wald, 1972; Kado, 1973), heterogeneity of excitability of the somatic membrane has not been investigated experimentally, because intracellularly induced currents depolarize the somatic membrane homogeneously. By changing the direction of application of extracellular current in our experiments, it was possible to localize zones of action potential generation in the process and in the soma. In vertebrate neurones, action potentials are usually generated on the axon hillcok (Coombs *et al.* 1957*a*,*b*), and their thresholds are lower than the threshold of the soma. Several zones of action potential generation can exist in dendrites (Fadiga & Brookhart, 1960; Kuno & Llinas, 1970). In invertebrate

neurones, zones of action potential generation are located at the point of process branching (Tauc, 1962*a*,*b*; Tauc & Hughes, 1963). Some authors consider these regions as pacemaker zones (Mayeri, 1973; Treistman, 1980), but in experiments on isolated neurones, the pacemaking ability of a soma without processes has been demonstrated (Alving, 1968). Our data confirm the existence of several zones of action potential generation in the cell, and show that localized areas of somatic membrane possess the ability to generate pacemaker potentials.

REFERENCES

ALVING, B. O. (1968). Spontaneous activity in isolated somata of *Aplysia* pacemaker neurones. *J. gen. Physiol.* **51**, 29–45.

ARVANITAKI, A. (1942). Effects evoked in an axon by the activity of a contiguous one. *J. Neurophysiol.* **5**, 89–108.

BERNHARDT, J. & PAULY, H. (1973). On the generation of potential differences across the membranes of ellipsoidal cells in an alternating electrical field. *Biophysics* **10**, 89–98.

BINDMAN, L. J., LIPPOLD, O. C. J. & REDFEARN, J. W. T. (1964). The action of brief polarizing currents on the cerebral cortex of the rat (1) during current flow and (2) in the production of long-lasting aftereffects. *J. Physiol., Lond.* **172**, 369–382.

BROWN, M. C. & MATTHEWS, P. B. C. (1960). The effect on a muscle twitch of the back-response of its motor nerve fibres. *J. Physiol., Lond.* **150**, 332–346.

COOMBS, J. S., CURTIS, D. R. & ECCLES, J. C. (1957*a*). The interpretation of spike potentials of motoneurones. *J. Physiol., Lond.* **139**, 198–231.

COOMBS, J. S., CURTIS, D. R. & ECCLES, J. S. (1957*b*). The generation of impulses in motoneurones. *J. Physiol., Lond.* **139**, 232–249.

CREUTZFELDT, O. D., FROMM, G. H. & KAPP, H. (1962). Influence of transcortical D-C currents on cortical neuronal activity. *Expl Neurol.* **5**, 436–452.

FADIGA, E. & BROOKHART, J. M. (1960). Monosynaptic activation of different portions of the motor neurone membrane. *Am. J. Physiol.* **198**, 693–703.

FURUKAWA, T. & FURSHPAN, E. J. (1963). Two inhibitory mechanisms in the Mauthner neurons of goldfish. *J. Neurophysiol.* **26**, 140–176.

GRANIT, R. & PHILLIPS, C. G. (1957). Effects on Purkinje cells of surface stimulation of the cerebellum. *J. Physiol., Lond.* **135**, 73–92.

JEFFERYS, J. G. R. (1981). Influence of electric fields on the excitability of granule cells in guinea-pig hippocampal slices. *J. Physiol., Lond.* **319**, 143–152.

KADO, R. T. (1973). *Aplysia* giant cell: soma–axon voltage clamp current differences. *Science* **182**, 843–845.

KATER, S. B. & HADLEY, R. D. (1982). Intracellular staining combined with video fluorescence microscopy for viewing living identified neurons. In *Cytochemical Methods in Neuroanatomy*. New York: Alan. R. Liss., Inc. 441pp.

KUNO, M. & LLINAS, R. (1970). Enhancement of synaptic transmission by dendritic potentials in chromatolysed motoneurones of the cat. *J. Physiol., Lond.* **210**, 807–821.

MAYERI, E. (1973). Functional organization of the cardiac ganglion of the lobster (*Homarus americanus*). *J. gen. Physiol.* **62**, 448–472.

RAMON, F. & MOORE, J. W. (1978). Ephaptic transmission in squid giant axons. *Am. J. Physiol.* **234**, c162–c169.

RICHARDSON, T. L., TURNER, R. W. & MILLER, J. J. (1984). Extracellular fields influence transmembrane potentials and synchronization of hippocampal neuronal activity. *Brain Res.* **294**, 255–262.

SACHAROV, D. A. (1974). *Genealogy of Neurones* (in Russian). Moscow: Nauka.

TAUC, L. (1962*a*). Site of origin and propagation of the spike in the giant neuron of *Aplysia*. *J. gen. Physiol.* **45**, 1077–1097.

TAUC, L. (1962*b*). Identification of active membrane areas in the giant neuron of *Aplysia*. *J. gen. Physiol.* **45**, 1099–1115.

TAUC, L. & HUGHES, G. M. (1963). Modes of initiation and propagation of spikes in the branching axons of molluscan central neurons. *J. gen. Physiol.* **46**, 533–549.

TERZUOLO, C. A. & BULLOCK, T. H. (1956). Measurement of imposed voltage gradient adequate to modulate neuronal firing. *Proc. natn. Acad. Sci. U.S.A.* **42**, 687–694.

TREISTMAN, S. N. (1980). Axonal site for impulse initiation and rhythmogenesis in *Aplysia* pacemaker neurons. *Brain Res.* **187**, 201–205.

WALD, F. (1972). Ionic differences between somatic and axonal action potentials in snail giant neurones. *J. Physiol., Lond.* **220**, 267–281.